Advances in Renewable Energies Offshore – Guedes Soares (Ed.)
© 2019 Taylor & Francis Group, London, ISBN 978-1-138-58535-5

Parametric motion detection for an oscillating water column spar buoy

G. Giorgi & J.V. Ringwood
Centre for Ocean Energy Research, Maynooth University, Ireland

ABSTRACT: Parametric resonance is a highly nonlinear phenomenon, difficult to model and foresee, with often detrimental consequences on the power production efficiency of wave energy converters. Parametric excitation, due to time-varying parameters of the system, activates an internal excitation mechanism, which diverts part of the energy from the principal degree of freedom, consequently generating parasitic motions. Although the ability of a mathematical model to articulate parametric instability is beneficial for design and control purposes, the increase in computational burden and complexity is often unacceptable. However, using computationally frugal nonlinear Froude-Krylov force calculations, applicable to axisymmetric devices, it is possible to define mathematical models fast enough for computation in real time. The focus of the paper is a floating oscillating water column device, inspired by the Sparbuoy device, in order to demonstrate the ability of such a mathematical model to describe parametric roll responses.

1 INTRODUCTION

Exact and representative mathematical models are of paramount importance for effective design and optimization of wave energy converters (WECs). Although, in the wave energy community, linear models are predominantly implemented, thanks to their simplicity and computational convenience, they often provide a poor description of the dynamical behaviour of the system, far from being an accurate representation of the actual response of the device. Indeed, conditions for linearity are seldom met, in wave energy applications, since the purpose of maximising power extraction requires to exaggerate the motion, consequently enhancing nonlinear effects (Giorgi and Ringwood, 2017b).

One remarkable example of extremely nonlinear phenomenon, undetectable by linear models, is parametric resonance, which consists of an internal excitation mechanism, diverting a portion of the incoming energy away from the main degree of freedom, namely the one where wave energy is converted. Therefore, if not expressly exploited, parametric excitation is effectively a source of energy loss, eventually reducing the overall conversion efficiency. Consequently, the ability to model and predict such a phenomenon is valuable for both design and control purposes, so that parametric resonance can be prevented, or even taken advantage of (Olvera et al., 2007). Furthermore, parametric motion should also be taken into account for survivability considerations, since excessive parametric motion may jeopardize the device integrity (Tarrant and Meskell, 2016).

Since parametric resonance is due to time-varying system parameters (Fossen and Nijmeijer, 2012), linear models, which take the mean wetted surface into account, are inadequate. In contrast, it has been shown that parametric instability can be detected by nonlinear Froude-Krylov (FK) models, which integrate the static and dynamic pressure of the undisturbed wave field over the *instantaneous* wetted surface. Particular examples, in wave energy applications, are given by the SEAREV (Babarit et al., 2009) and the Wavebob (Tarrant and Meskell, 2016) devices, for which parametric resonance is a detrimental parasitic effect, studied with a mesh-based nonlinear FK force model (LAMSWEC) (Gilloteaux, 2007), which compares well with wave tank tests, provided an appropriate viscous drag description is included. Nonetheless, the main drawback of mesh-based nonlinear FK models is the computational time, since they require time-consuming re-meshing routines.

However, while mesh-based approaches are likely to be the only option for a geometry of arbitrary complexity, a computationally efficient method is available for axisymmetric devices (Giorgi and Ringwood, 2017a). Note that the symmetry of revolution assumption is not particularly restrictive for point absorbers, since they are usually designed to be non-directional, therefore axisymmetric. In this paper, an oscillating water column (OWC) spar buoy is considered, inspired by the Sparbuoy device (Gomes et al., 2017), since wave tank tests have shown such a device to be particularly prone to parametric resonance.

The remainder of the paper is organized as follows: Sect. 2 presents the nonlinear mathematical model, while Sect. 3 describes the device configuration and parameters. Some results are presented in Sect. 4, while Sect. 5 gives concluding remarks and considerations.

2 MATHEMATICAL MODEL

Two right-handed frames of reference are introduced: an inertial frame (x, y, z), with the origin at the still water level (SWL), x pointing in the direction of propagation of the wave, and z pointing upwards; and a non-inertial frame $t(\hat{x},\hat{y},\hat{z})$, fixed with the body, with the origin at the centre of gravity of the body. Assuming the fluid to be inviscid, and the flow to be irrotational and incompressible, linear potential theory can be formulated, defining the equation of motion for a generic single body, in the body-fixed frame of reference, as:

$$M\ddot{\mathbf{x}} = \mathbf{f}_{FK_{st}} + \mathbf{f}_{FK_{dy}} + \mathbf{f}_{d} + \mathbf{f}_{rad} + \mathbf{f}_{vis} + \mathbf{f}_{moor} + \mathbf{f}_{PTO}, \quad (1)$$

where M is the inertial matrix, $\mathbf{x} = (\hat{x},\hat{y},\hat{z},\phi,\theta,\psi)$ is the state vector in the body-fixed frame, $\mathbf{f}$ are the generalized force vectors, composed of 3 forces ($\mathbf{F}$), and 3 torques ($\mathbf{T}$). The force components on the right hand side of (1) are the static and dynamic FK forces $\mathbf{f}_{FK_{st}}$ and $\mathbf{f}_{FK_{dy}}$, respectively, the diffraction force $\mathbf{f}_{d}$, the radiation force $\mathbf{f}_{rad}$, the viscous force $\mathbf{f}_{vis}$, the mooring force $\mathbf{f}_{moor}$, and the power take-off (PTO) force $\mathbf{f}_{PTO}$.

The mooring system is potentially an important factor for generation of parametric instability, according to the particular mooring configuration (Davidson and Ringwood, 2017). Likewise, the viscous drag force, may be essential in nonlinear FK force models, to avoid unrealistic magnification of the motion, when parametric instability appears (Babarit et al., 2009). In this paper, linear radiation and diffraction forces are considered, which is a reasonable approximation for devices much smaller than the characteristic wave length (Falnes, 2002). A computationally convenient state space representation has been used to model radiation forces, based on a moment-matching technique (Faedo et al., 2017).

Froude-Krylov forces correspond to the integral of the pressure of the undisturbed incident wave field, over the wetted surface of the device. Such a pressure is defined, according to linear Airy's theory, as:

$$p(x,z,t) = p_{st} + p_{dy} = -\gamma z + \gamma \frac{cosh\left(k(z+h)\right)}{cosh\left(kh\right)}\eta(x,t) \quad (2)$$

where $p_{st} = -\gamma z$ is the static pressure, p_{dy} the dynamic pressure, γ the specific weight of sea water, $\eta(x,t)$ a 2-dimensional wave with amplitude $a = H_w/2$ and wave period T_w, k the wave number, and h the water depth. It is also convenient to apply Wheeler stretching to (2), as shown in (Giorgi and Ringwood, 2018b).

Froude-Krylov forces ($\mathbf{F}_{FK}$) and torques ($\mathbf{T}_{FK}$) are computed by integrating the pressure, shown in (2), over the instantaneous wetted surface $S(t)$:

$$\mathbf{F}_{FK_{st}} + \mathbf{F}_{FK_{dy}} = \mathbf{F}_{g} + \iint_{S(t)} p_{st}\mathbf{n}dS + \iint_{S(t)} p_{dy}\mathbf{n}dS \quad (3a)$$

$$\mathbf{T}_{FK_{st}} + \mathbf{T}_{FK_{dy}} = \mathbf{r}\times\mathbf{F}_{g} + \iint_{S(t)} p_{st}\mathbf{r}\times\mathbf{n}dS + \iint_{S(t)} p_{dy}\mathbf{r}\times\mathbf{n}dS \quad (3b)$$

where $\mathbf{F}_{g}$ is the gravity force, $\mathbf{n} = (n_x, n_y, n_z)$ is the unit vector normal to the surface, pointing outwards, $\mathbf{r}$ is the position vector, and $\times$ is the cross product.

Under linear approximation, a constant wetted surface is considered, in integrals (3) and (4), relying on the assumption of small relative motion between the wave and the device. In contrast, nonlinear FK forces are computed with respect to the *instantaneous* wetted surface, therefore taking the real position of the device, with respect to η, into account.

For a geometry of arbitrary complexity, the actual calculation of the nonlinear FK integrals requires the use of plane panels to discretize the surface, which consequently has to be remeshed, at every time step, in order to define the instantaneous wetted surface (Gilloteaux, 2007). Such a remeshing routine makes the approach computationally expensive. However, for *axisymmetric* buoys, a convenient parameterization of the wetted surface can ease the calculation of the FK integrals. Such a method, described hereafter, is validated in (Giorgi and Ringwood, 2018a).

The assumption of an axisymmetric geometry allows an analytical description of the complete wetted surface, therefore avoiding computationally expensive mesh-based techniques. The geometry of a generic buoy, symmetric around a vertical axis, can be described in cylindrical coordinates, with respect to the body-frame $(\hat{x},\hat{y},\hat{z})$, as follows:

$$\begin{cases} \hat{x}(\varrho,\vartheta) = f(\varrho)\cos\vartheta \\ \hat{y}(\varrho,\vartheta) = f(\varrho)\sin\vartheta \\ \hat{z}(\varrho,\vartheta) = \varrho \end{cases}, \quad \theta \in [-\pi,\pi] \wedge \varrho \in [\varrho_1,\varrho_2] \quad (4)$$

where $f(\vartheta)$ is a generic function of the vertical coordinate ϱ, describing the profile of revolution

of the axisymmetric body, as shown in (Giorgi and Ringwood, 2017b).

The change of coordinates, from Cartesian $(\hat{x},\hat{y},\hat{z})$ to cylindrical (ϱ,ϑ), shown in (5), requires the inclusion of $\left\|\mathrm{e}_{\varrho}\cdot\mathrm{e}_{\vartheta}\right\|$ in the integral, where e_{ϱ} and e_{ϑ} are unit vectors in the ϱ and ϑ directions, respectively. Furthermore, $\mathbf{n}$ can be expressed as $\frac{\mathrm{e}_{\varrho}\cdot\mathrm{e}_{\vartheta}}{\left\|\mathrm{e}_{\varrho}\cdot\mathrm{e}_{\vartheta}\right\|}$. Finally, since the integrals are defined in the body frame, it is necessary to map the pressure from the inertial-frame (where it is defined) onto the body surface. The transformation, from $(x,\ y,\ z)$ to $(\hat{x},\hat{y},\hat{z})$, is represented by the Euler angle triad (ϕ,θ,ψ), corresponding to roll, pitch, and yaw angles, respectively. The 3-2-1 Euler angle sequence is the rotation convention commonly used for marine vehicles, thought of as three sets of rigid rotations (Fossen, 2011). In order to apply a rotation around the origin of the body frame (instead of around the origin of the inertial frame), a translation needs to be applied before and after the rotation, so that the two origins overlap at the moment of the rotation. Consequently, the integral for $\mathbf{F}_{FK_{dy}}$ in (3), for example, becomes:

$$\begin{aligned}\mathbf{F}_{FK_{dy}} &= \iint_{S(t)} p_{dy}(\hat{x},\hat{y},\hat{z})\,n\,dS \\ &= \int_{\vartheta_1}^{\vartheta_2}\int_{\varrho_1}^{\varrho_2} p_{dy}(\varrho,\vartheta)\,\mathbf{e}_{\varrho}\times\mathbf{e}_{\vartheta}\,d\varrho\,d\vartheta\end{aligned} \tag{5}$$

Although such an approach is applicable to any geometry with symmetry of revolution, the vast majority of axisymmetric point absorbers can be described as a combination of cylinders, cones, and spheres. Note that discs (lids), which close the surface of a cylinder, cannot be described using cylindrical coordinates. To this end, polar coordinates are valid alternatives to cylindrical, as shown in (Giorgi and Ringwood, 2018a).

Finally, the FK force integrals must be solved numerically using, for example, a trapezoidal rule. The computation time depends on the integration scheme utilized, a 2D-quadrature scheme (Shampine, 2008), and on the relative and absolute tolerances used to approximate the integral, both set to 10^{-3}. The ultimate value of the computation time depends on hardware capabilities (Intel(R) Xeon(R) CPU (E5–1620 v3 @ 3.50 GHz) processor, with 16.0 GB RAM and Windows 7 Professional 64 bit), on the complexity of the geometry, and on the number of bodies and degrees of freedom (DoFs) considered. For the device studied in this paper, described in Sect. 3, the calculation time for the nonlinear FK forces, is between $1{\cdot}10^{-2}$ *s* and $4{\cdot}10^{-2}$ *s*, at a single time instant. The consequent run time for computing the response of the device depends on the discrete time solver scheme, the time step, and the simulation duration. Using a constant time step second-order Runge-Kutta scheme, varying the time step from 0.005*s* to 0.025*s*, for a regular wave of period about 0.7*s*, the resulting run time is between one and three times the simulation time. Therefore, such a method has the potential to run roughly in real time, or a little slower, depending on the particular implementation. However, the computation times given are for computations performed in Matlab, which is between one and two orders of magnitude slower than lower level coding languages, such as C or Fortran (Wendt et al., 2017). With C or Fortran implementation, therefore, real time execution is easily achievable. Nevertheless, although the mesh-based LAMSWEC nonlinear FK model is coded in Fortran (which is a significantly faster implementation than Matlab), it has a run time about 10 times longer than the simulation time (Gilloteaux, 2007), therefore about one order of magnitude slower than the method used in this paper.

3 SPARBUOY MODEL

The device studied in this paper is inspired by the Sparbuoy WEC (Gomes et al., 2017), which is a floating OWC, extracting energy from the relative motion between a hollow spar buoy and the water column contained within. The 1:100 scale prototype is considered, for which wave tank experiments highlight parametric resonance (Gomes et al., 2017). The shape and dimensions of the floater are shown in Fig. 1, while Table 1 tabulates relevant physical quantities (z_g the center of gravity, z_b the center of buoyancy, m the mass of the floater, I the roll/pitch inertia, and T_n the natural period). Moorings are modelled, in surge and sway, as linear restoring coefficients, chosen in order to match the surge natural period, given in (Gomes et al., 2017).

Mooring forces are known to, potentially, play an important role in parametric resonance generation, as discussed in (Davidson and Ringwood, 2017). However, since the purpose of the present paper is to show the ability of the nonlinear FK model to articulate *hydrodynamically* induced parametric roll, the mooring model has been extremely simplified.

The Sparbuoy device can be modelled as a two-body system, considering the floater in 6-DoFs, and an additional heaving DoF for the water column, effectively modelled as a weightless rigid piston (Henriques et al., 2016). The hydrodynamic coefficients are computed with the boundary element method software WAMIT, using generalized modes for the moonpool free surface (WAMIT Inc., 2014).

A linear air turbine is considered, for which the ratio between the pressure difference in the chamber and the flow rate is constant (k_{PTO}). Ignoring

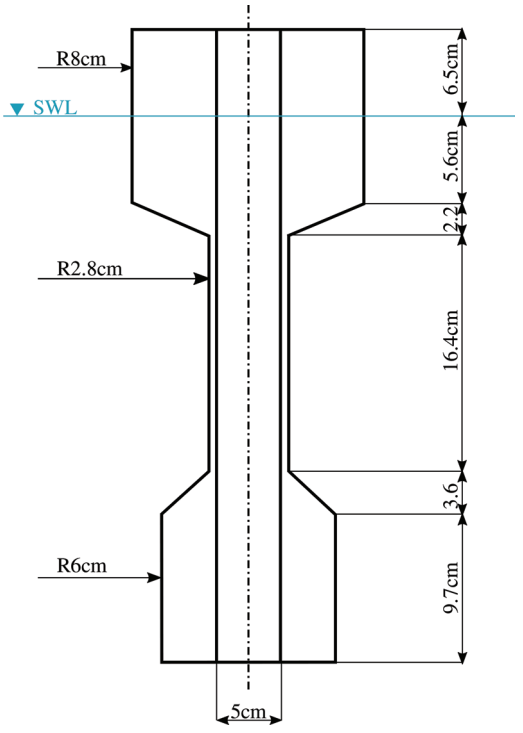

Figure 1. Shape and dimensions of the Sparbuoy-like device, at 1:100 prototype scale.

Table 1. Physical properties of the Sparbuoy-like device, at 1:100 prototype scale. Coordinates given in the inertial frame.

			Surge		Roll
			Sway	Heave	Pitch
z_g	$[m]$	–0.205			
z_b	$[m]$	–0.168			
m	$[kg]$	2.395			
I	$[kg/m^2]$	0.00733			
T_n	$[s]$		12.7	0.89	1.35

air compressibility effects (Sheng et al., 2015), it follows that the force exchanged between the water column and the floater is:

$$F_{PTO} = \pm k_{PTO} A_{wc}^2 \left(\dot{\mathbf{x}}(3) - \dot{\mathbf{x}}(7) \right), \tag{6}$$

where A_{wc} is the cross sectional area of the water column, $\dot{\mathbf{x}}$ is the heave velocity of the floater ($\dot{\mathbf{x}}(3)$) and the water column ($\dot{\mathbf{x}}(7)$), respectively. The symbol ± means that F_{PTO} acts on the two bodies with opposite sign. The turbine coefficient is optimized for each wave condition, using the linear model, in order to maximise power capture (Sheng et al., 2015).

With the aim of defining a parsimonious model, nonlinear computation of FK forces are applied only to the floater's heave, roll, and pitch DoFs, since in (Giorgi and Ringwood, 2018a) it is suggested that a nonlinear description of surge and sway is likely to be of little additional value in terms of accuracy, compared to the other DoFs. Nonlinear heave and pitch calculations can be validated against WAMIT results (for modest device motion), as shown in Fig. 2, computing, in linear conditions, heave and pitch excitation force coefficients, $\bar{\mathbf{f}}_{ex}(3)$ and $\bar{\mathbf{f}}_{ex}(5)$, respectively. In fact, nonlinearities are negligible if the floater is kept in place, and the incoming wave is extremely small ($H_w = 10^{-6}\, m$); in such conditions, linear and nonlinear results overlap. Likewise, the hydrostatic stiffness coefficients have been verified, by computing the nonlinear force/torque after an infinitesimal displacement, in the complete absence of waves.

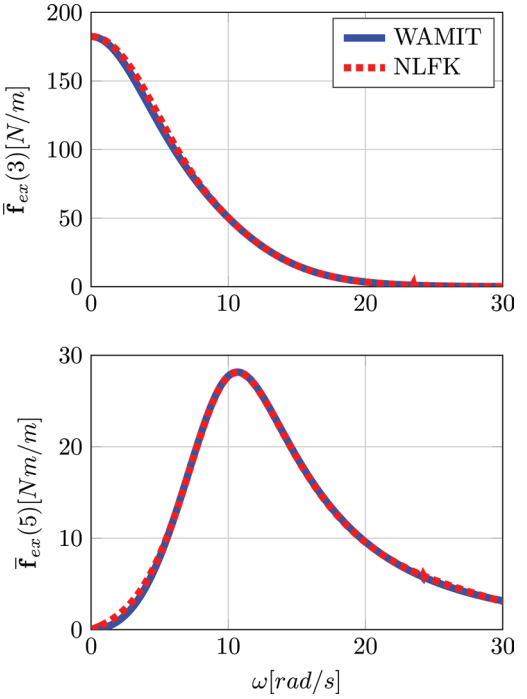

Figure 2. Validation, against WAMIT results and in linear conditions ($H_w = 10^{-6}\, m$), of nonlinear Froude-Krylov (NLFK) calculations of excitation coefficients in heave and pitch.

4 RESULTS

Parametric instability is well-known to appear when two conditions are verified (Fossen and Nijmeijer, 2012): the amplitude of the excitation is larger than the damping of the secondary DoF, and the frequency of external excitation is about twice the natural frequency of the parametrically excited DoF. Therefore, in order to study the amplitude and the frequency conditions separately, simulations have been performed using a dense grid of wave conditions, with 11 wave heights, equally spaced between 0.005 m and 0.0150 m, and 76 wave periods, equally spaced between 0.5 s and 2 s.

Dissipation mechanisms, in the roll DoF, are the radiation damping and the viscous drag (which is modelled as an additional linear loss, proportional to the velocity) losses. Due to the lack of accurate information regarding the determination of a viscous drag coefficient, it is initially set to zero, and then a sensitivity analysis is performed. The resulting maximum roll response, without drag, is shown in Fig. 3.

It is noteworthy that the nonlinear FK model is indeed able to articulate the highly-nonlinear phenomenon of hydrodynamic parametric resonance which, in this case study, is the only possible source of generating a response in the roll DoF. Furthermore, as predicted by theory (Fossen and Nijmeijer, 2012), and consistent with experimental results (Gomes et al., 2017), parametric roll is sharply localized at wave periods equal to or half of the roll natural period, while elsewhere the roll response is null. Likewise, it can be noted that parametric instability kicks in after an amplitude threshold is passed, namely for a 0.009 m heighs wave, at $T_w = 0.5T_n$.

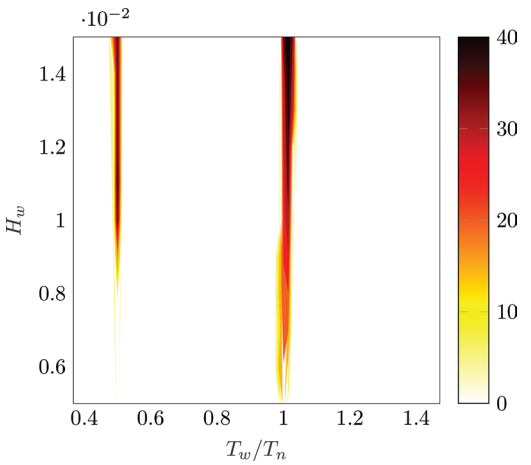

Figure 3. Maximum roll response, in degrees, without viscous drag. Wave periods are normalized by the roll natural period.

Further insight can be gained by analysing the spectral energy content of the response of the device, both in roll and pitch. Considering, by way of example, a representative wave height of 0.01 *m*, the Fourier transform is computed for all wave periods, as shown in the waterfall plots in Fig. 4 and Fig. 5, for roll and pitch, respectively. Both the Fourier frequency components (ω), and the excitation frequencies (ω_e), are normalized by the roll natural frequency (ω_n).

Considering Fig. 4, it is clear that the roll response is nonzero only for normalized excitation frequencies of 1 and 2, and the spectra contain has an evident peak at the normalized frequency component of 1. In fact, while the roll degree of freedom is never externally excited, parametric resonance activates an internal excitation mechanism at integer multiples of the normalized excitation frequency.

Conversely, since waves are externally exciting the device in the pitch DoF, the spectra of the

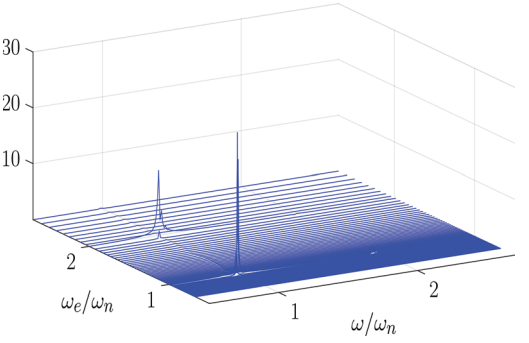

Figure 4. Magnitude of the Fourier transforms of the roll response, in degrees, at different excitation frequencies ω_e, with wave amplitude of 0.01 *m*. Both frequencies are normalized by the roll natural frequency (ω_n).

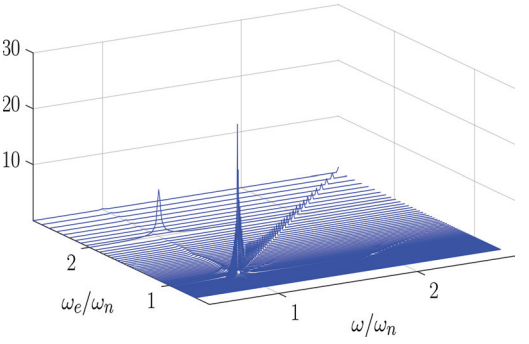

Figure 5. Magnitude of the Fourier transforms of the pitch response, in degrees, at different excitation frequencies ω_e, with wave amplitude of 0.01 *m*. Both frequencies are normalized by the roll natural frequency (ω_n).

response shows a peak at the same excitation frequency; indeed, Fig. 5 shows that peaks align along the bisector of the horizontal plane (direction $\omega = \omega_e$). Looking at the plot from the perpendicular direction of the diagonal (direction $\omega = -\omega_e$), one can recognize the typical shape of the first-order pitch response. However, for a normalized excitation frequency of 2, when parametric roll happens, a peak in the pitch spectra is generated at the pitch natural frequency.

From the discussion so far, it is clear that parametric resonance is an extremely frequency-dependent phenomenon. Regular waves steadily excite the device at the same frequency, facilitating the progressive build-up of parametric instability, when the excitation frequency is equal to, or twice, the resonant frequency. However, real waves are panchromatic, so conditions for parametric excitation are weaker. Figure 6 shows an example of the roll response, subject to an irregular wave realization of a JONSWAP spectrum, with a peak enhancing factor of 5, significant wave height $H_s = 0.015\ m$, and peak period $T_p = 0.68\ s$.

Figures 3 to 6 demonstrate that the model is able to articulate parametric instability. However, in spite of the fact that the likelihood of, and the conditions for, parametric generation are well described, the severity of the parametric response is overestimated. In fact, although the model considered in this paper has simplified mooring and PTO systems, with respect to the one tested in (Gomes et al., 2017), making the comparison less relevant, the maximum roll response obtained in the wave tank is about 21 degrees, about half that obtained here. Such a result is consistent with the absence of viscous drag loss in the model for rotational DoFs. A similar issue is found, for example, in (Babarit et al., 2009), where the LAMSWEC (mesh-based nonlinear FK) method is applied to the SEAREV device, without modelling viscous drag effects.

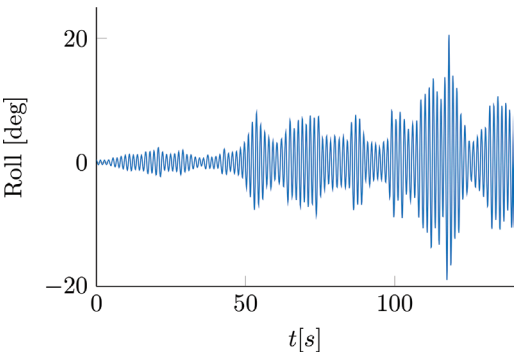

Figure 6. Roll response, without drag, to an irregular wave with $H_s = 0.015\ m$ and $T_p = 0.68\ s$.

Therefore, in order to discuss the influence of viscous drag on the generation of parametric resonance, a sensitivity study is performed. Considering a wave at half the pitch natural period (0.68 s), and $H_w = 0.01\ m$, 11 linear drag coefficient values are used, equally spaced between 0 and $0.01 Nms$. The resulting time traces are shown in Fig. 8, where each area represents the envelope of a time trace, using one drag coefficient value, while the amplitudes of the steady state responses are shown in Fig. 7.

As expected, larger linear drag coefficients cause the roll response to diminish, until it effectively disappears for a drag coefficient of $0.01 Nms$. In fact, one of the usual solutions adopted, in order to avoid parametric roll, is to increase viscous dissipation, for example through additional fins attached to the main floater body (Gomes et al., 2017). However, Fig. 8, which plots simulation results of

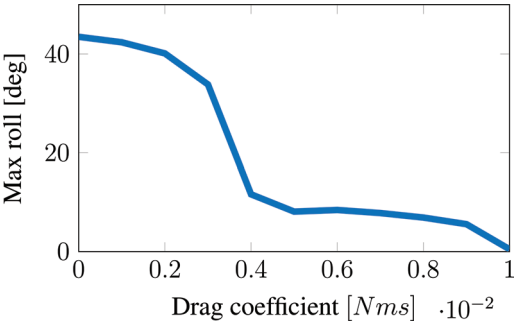

Figure 7. Amplitudes of the steady state roll responses, for a wave with $T_w = 0.68\ s$ and $H_w = 0.01\ m$, for 11 linear drag coefficients, equally spaced between 0 and 0.01 *Nms*.

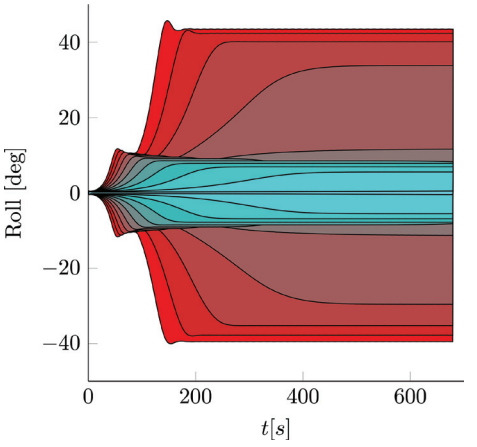

Figure 8. For a wave with $T_w = 0.68\ s$ and $H_w = 0.01\ m$, for 11 linear drag coefficients, equally spaced between 0 and $0.01 Nms$, each area corresponds to the envelop of the roll response time traces. As drag increases, roll response decreases.

1000 wave periods long, shows also that the transient period for building-up steady parametric roll significantly increases with the drag coefficient value. Consequently, a very long transient in regular wave conditions would reduce the significance of parametric resonance in real sea conditions: given the panchromatic nature of irregular waves, there would be insufficient time to generate a sustained parametric response.

5 CONCLUSIONS

Parametric resonance is a highly-nonlinear phenomenon, often unexpected by wave energy converter designers. In fact, at an early design stage, when significant modifications to the device concept, operating principle, shape, and dimensions take place, over-simplistic linear models are commonly used, due to their computational convenience. However, parametric resonance, undetectable by linear models, is usually discovered (with some dismay!) after the first wave tank tests, at a stage where there is less design freedom, due to the larger financial investment needed. Therefore, since parametric roll is usually detrimental, suboptimal mitigating actions take place, in order to contain the undesired phenomenon.

On the contrary, having a computationally viable mathematical model, able to describe nonlinearities, including parametric resonance, is potentially beneficial for informing the design process of the *real* device dynamics. Furthermore, reliable knowledge of the device dynamics can eventually channel the device design into exploiting nonlinear behaviours, instead of limiting them. In particular, since instability is an extreme magnification of a small perturbation, a dedicated design that takes advantage of parametric resonance is potentially highly beneficial for power production. A well informed control strategy may exploit parametric resonance in order to generate the conditions for maximum power generation.

Such device/control design approaches require a *fast* and *representative* model of the device. The present paper takes a step in this direction, implementing a computationally convenient modelling approach for nonlinear Froude-Krylov force calculation for an axisymmetric wave energy converter, able to compute almost in real time, despite a relatively slow coding language, but already an order of magnitude faster than previous similar models. The ability of such a method to articulate parametric excitation is demonstrated by considering a Sparbuoy-like device, known to have a parametric response. Such a mathematical model can be useful for design investigations, for example exploring the sensitivity of parametric roll generation to viscous drag variations.

ACKNOWLEDGEMENTS

This paper is based upon work supported by Science Foundation Ireland under Grant No. 13/IA/1886.

REFERENCES

Babarit, A., H. Mouslim, A.H. Clément, & P. Laporte-Weywada (2009). On the numerical modelling of the nonlinear behavior of a wave energy converter. In *Proceedings of the ASME 2009 28th International Conference on Ocean, Offshore and Arctic Engineering, May 31 – June 5*.

Davidson, J. & J.V. Ringwood (2017). Mathematical modelling of mooring systems for wave energy converters – A review. *Energies 10*(5).

Faedo, N., Y. Peña-Sanchez, & J.V. Ringwood (2017). Finite-Order Hydrodynamic Model Determination for-Wave Energy Applications Using Moment-Matching. *submitted to Ocean Engineering*.

Falnes, J. (2002). *Ocean waves and oscillating systems*. Cambridge University Press.

Fossen, T.I. (2011). *Handbook of marine craft hydrodynamics and motion control*. John Wiley & Sons.

Fossen, T.I. & H. Nijmeijer (2012). *Parametric resonance in dynamical systems*. Springer.

Gilloteaux, J.-C. (2007). *Mouvements de grande amplitude d'un corps flottant en fluide parfait. Application á la recuperationd de l'energie des vagues*. Ph. D. thesis, Ecole Centrale de Nantes-ECN.

Giorgi, G. & J.V. Ringwood (2017a). Computationally efficient nonlinear Froude–Krylov force calculations for heaving axisymmetric wave energy point absorbers. *Journal of Ocean Engineering and Marine Energy 3*(1), 21–33.

Giorgi, G. & J.V. Ringwood (2017b). Froude-Krylov and Viscous Drag Representations in Nonlinear Wave Energy Devices Models in the Computation/Fidelity Continuum. *Ocean Engineering 141*, 164–175.

Giorgi, G. & J.V. Ringwood (2018a). Analytical representation of nonlinear Froude-Krylov forces for 3-DoF point absorbing wave energy devices. *submitted to Ocean Engineering*.

Giorgi, G. & J.V. Ringwood (2018b). Relevance of pressure field accuracy for nonlinear Froude Krylov force calculations for wave energy devices. *Journal of Ocean Engineering and Marine Energy 4*(1), 57–71.

Gomes, R.P.F., J.D.C. Malvar Ferreira, S. Riberio de Silva, J.C. Henriques, & L.M.C. Gato (2017). An experimental study on the reduction of the dynamic instability in the oscillating water column spar buoy. In *12th European Wave and Tidal Energy Conference (EWTEC), Cork*, Number August.

Henriques, J.C., J.C. Portillo, L.M.C. Gato, R.P.F. Gomes, D.N. Ferreira, & A.F. Falčao (2016). Design of oscillating water-column wave energy converters with an application to self-powered sensor buoys. *Energy 112*, 852–867.

Olvera, A., E. Prado, & S. Czitrom (2007). Parametric resonance in an oscillating water column. *Journal of Engineering Mathematics 57*(1), 1–21.

Shampine, L.F. (2008). Matlab program for quadrature in 2D. *Applied Mathematics and Computation 202*(1), 266–274.

Sheng, W., R. Alcorn, & A. Lewis (2015). Hydrodynamics of OWC wave energy converters. *Renewable Energies Offshore*, 489–496.

Tarrant, K.R. & C. Meskell (2016). Investigation on parametrically excited motions of point absorbers in regular waves. *Ocean Engineering*.

WAMIT Inc., M.I.T. (2014). User Manual Wamit.

Wendt, F.F., Y.-H. Yu, K. Nielsen, K. Ruehl, T. Bunnik, I. Touzon, B.W. Nam, J.S. Kim, K.-H. Kim, & C.E. Janson (2017). International Energy Agency Ocean Energy Systems Task 10 Wave Energy Converter Modeling Verification and Validation. In *12th European Wave and Tidal Energy Conferenc European Wave and Tidal Energy Conference*. Technical Committee of the European Wave and Tidal Energy Conference.